International Journal of Power Electronics and Drive System (IJPEDS)
Vol. 8, No. 2, June 2017, pp. 945~956
ISSN: 2088-8694, DOI: 10.11591/ijpeds.v8i2.pp945-956

Efficient Approach to LVRT Capability of DFIG-Based Wind Turbines under Symmetrical and Asymmetrical Voltage Dips Using Dynamic Voltage Restorer

Kiarash Azizi[1], Murtaza Farsadi[2], Mohammad Farhadi Kangarlu[3]
Department of Electrical and Computer Engineering, Urmia University, Iran

Article Info

Article history:

Received Feb 10, 2017
Revised Apr 10, 2017
Accepted Apr 24, 2017

Keyword:

(DVR)
Doubly fed induction generator (DFIG)
Dynamic Voltage Restorer
Low-voltage ride-through (LVRT)
Symmetrical and asymmetrical voltage dips

ABSTRACT

The capability of low-voltage ride-through (LVRT) of doubly fed induction generator (DFIG) has been considered as an essence for grid code requirements. Any unbalance on the grid side causes the rotor current of the generator to rise which leads to saturate the dc-link of the back-to-back converter or even destroy it. To meet this requirement, a dynamic voltage restorer (DVR) without dc-link energy storage elements is utilized to compensate any disturbance imposed to the DFIG wind turbine system. On the time of any disturbance or fault, DFIG and DVR are properly controlled in order to compensate the specified faulty phase uninterruptedly. DVR is connected in series to the grid and by injecting instantaneous compensating voltage, prevents the stator voltage from rapid changing; consequently, the rotor side converter can accomplish its normal operation. As voltage dips are the most common grid faults subjected to DFIGs, this paper investigates both symmetrical and asymmetrical voltage dips caused by grid faults. The independent and instantaneous phase voltage compensation, less volume, weight, and cost are the merits to utilize the proposed DVR along with DFIG wind turbines. PSCAD/EMTDC based simulations verifies the capabilities of the proposed technique for the LVRT capability of DFIG.

Corresponding Author:

Kiarash Azizi,
Department of Electrical and Computer Engineering,
Urmia University, Urmia, Iran.
Email: st_k.azizi@urmia.ac.ir

1. INTRODUCTION

With increasing population, development, and distribution, as well as to keep pace with the growing need for new energy sources, more efficient with greater efficiency and with gradually ending fossil fuel, different renewable energy sources have been applied to meet these requirements. Among renewable energy sources like solar, wind, tidal, biomass and other potential sources wind energy plays a major role and has gained the fastest rate growth [1]. Low cost, less environmental effects, high efficiency, its infinite source, no greenhouse effect or acid rain are just some merits to consider wind energy as an important renewable wind energy. Wind turbines are usually divided into two categories:

a. Constant speed turbines (or up to 1 % speed)
b. Also known as fixed-speed Induction generator (FSIG).
c. Variable speed turbines

Such as: doubly fed induction generator (DFIG), wound field synchronous generator (WFSG), and permanent magnet synchronous generator (PMSG). Nowadays the major wind turbine systems are based on variable speed turbines. DFIG based wind turbine system has some advantages over other types which can be explained as follows [2-4]:

a. The sizes in DFIG have been larger
b. Their high ability to comply with grid code requirements
c. The induction generator used in fixed-speed wind turbines consumes reactive power which will include in employing capacitor banks
d. Reduced costs of converter and electromagnetic inference filter
e. lower electrical and thermal stress
f. Lower line current
g. For their constant frequency operating capability
h. Active and reactive power control ability.

These features make DFIG the most prominent wind turbine to be employed in power systems. These large types of wind turbines are installed in the on-shore and off-shore wind fields for producing megawatt power, meanwhile, small scaled power wind turbines are proper for the urban and residential areas [5-7].

Despite the mentioned merits, when DFIG is subjected to voltage dips it will bring great harm to the wind turbine system because the stator flux cannot follow sudden changes and will experience an unexpected change, at the same time as rotor keeps rotating and a high slip occurs it will provide condition for overvoltage and overcurrent in the rotor circuit. Under these circumstances, the rotor converter could be saturated and the control over the converter will be lost; it can also increase the induced electromagnetic force of the rotor, damage the converter, and increase the voltage in dc bus or causing oscillation in currents [8-12].

If no countermeasures are taken the wind turbine will trip and be disconnected from the power network, but the new grid codes require that wind turbines remain connected to the grid during voltage dips. The main objective is to avoid any disconnection of DFIG because of voltage dips. In order to achieve low voltage ride-through and protect the vulnerable converter of DFIG from overcurrent and overvoltage, various crowbar topologies can be employed [13-15]. The main problem with crowbar is the reactive power drawn from the power network which is against the grid code requirements. The final solution relies on using an external hardware like dynamic voltage restorer (DVR). Different topologies of DVR are proposed and utilized for DFIG-based wind turbine systems [16-19]. These proposed solutions use dc-link energy storage element which will result in embedding large capacitor in dc link. These types of DVR increase the cost and are not suitable for long time operation and their applications are limited. This paper presents an improved solution employing a DVR to achieve LVRT capability of DFIG-based wind turbine system with lower cost, less volume, less weight and independent voltage compensation.

2. DYNAMIC MODELLING OF DFIG UNDER VOLTAGE DIPS

A simplified schematic diagram of DFIG is shown in Figure 1. There are some publications focusing on the characteristics of DFIG during symmetrical and asymmetrical grid voltage conditions. Different types of these unbalance conditions which DFIGs are subjected and the control techniques to overcome these problems are presented in several papers [20-28]. This analysis is composed of two parts. In the first part normal operation of the DFIG will be analysed and the second part discusses the DFIG under voltage dips.

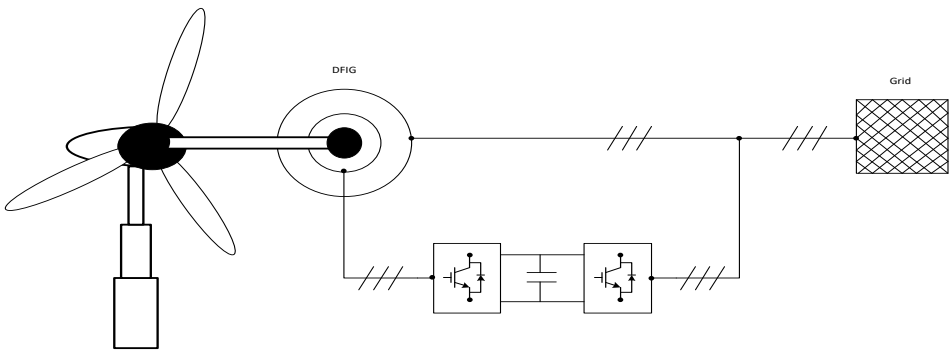

Figure 1. Simplified scheme of a DFIG

2.1. Normal Oeration of DFIG

Normal operation of DFIG is considered to have constant stator voltage in phase, amplitude and frequency the second part refers to the symmetric and asymmetrical voltage dips. The voltage equations of the DFIG can be represented by the following two equations:

$$\vec{v}_s^{\,s} = R_s \vec{i}_s^{\,s} + \frac{d\vec{\psi}_s^{\,s}}{dt} \tag{1}$$

$$\vec{v}_r^{\,r} = R_r \vec{i}_r^{\,r} + \frac{d\vec{\psi}_r^{\,r}}{dt} \tag{2}$$

where $\vec{v}_s^{\,s}$ and $\vec{i}_s^{\,s}$ are the stator voltage and current space vectors, $\vec{v}_r^{\,r}$ and $\vec{i}_r^{\,r}$ are the rotor voltage and current space vectors and $\vec{\psi}_s^{\,s}$ and $\vec{\psi}_r^{\,r}$ are stator and rotor flux space vectors, respectively. Equations (1) and (2) are represented in $\alpha\beta$(stator) and DQ(rotor) reference frames respectively; superscripts "s" and "r" indicate that space vectors are referred to stator and rotor reference frames. The stator and rotor flux equations related to the currents can be expressed as follows:

$$\vec{\psi}_s^{\,s} = L_s \vec{i}_s^{\,s} + L_m \vec{i}_r^{\,s} \tag{3}$$

$$\vec{\psi}_r^{\,r} = L_m \vec{i}_s^{\,r} + L_r \vec{i}_r^{\,r} \tag{4}$$

where L_s and L_r are the stator and rotor inductances with L_m being the magnetizing inductance. For the purpose of this paper, the park model is applied with the rotor variables referred to the stator. Equations (2) and (4) will be rewritten as follows (for simplicity superscripts "s" indicating static stator reference frame is omitted, so equations 1 and 3 could be ignored of rewriting):

$$\vec{v}_r = R_s \vec{i}_r + \frac{d\vec{\psi}_r}{dt} - j\omega_s \vec{\psi}_r \tag{5}$$

$$\vec{\psi}_r = L_r \vec{i}_r + L_m \vec{i}_s \tag{6}$$

where ω_s is the synchronous angular frequency. The rotor voltage owing to stator voltage can be expressed as:

$$\vec{v}_r = \vec{v}_s \frac{L_m}{L_s} s + \left(R_r + \sigma L_r \left(\frac{d}{dt} - j\omega_m \right) \right) \vec{i}_r \tag{7}$$

This is also the voltage generated by the converter where "s" is the slip ($s = \omega_r / \omega_s , \omega_r = \omega_s - \omega_m$) , σ is the leakage factor, ω_r and ω_m are the synchronous and electrical angular frequency; respectively. By neglecting the resistance R_r and the leakage factor σ (because of their small value), equation (7) will be more simplified:

$$\vec{v}_{rn} = j\omega_r \frac{L_m}{L_s} \vec{\psi}_s = \frac{\omega_r}{\omega_s} \frac{L_m}{L_s} V_s e^{j\omega_s t} \tag{8}$$

$$\vec{v}_{rn} = s \frac{L_m}{L_s} V_s e^{j\omega_s t} \tag{9}$$

$\vec{v}_{rn}$ Is the rotor voltage in which the term $s = L_m / L_s V_s$ will be considered as the amplitude of $\vec{v}_{rn}$, from Equation 9 it is obvious that the rotor voltage depends on stator voltage and the slip.

2.2. Symmetrical Voltage Dips

In the steady state, the stator flux is proportional to the stator voltage; that is, under a long enough time of voltage dip, the stator voltage will reach to zero and as it is a state variable, it will exponentially decrease to zero.

$$\vec{v}_{rn} = -\frac{L_m}{L_s}\left(\frac{1}{\tau_s} + j\omega_m\right)\vec{\Psi}_0 e^{-\frac{t}{\tau_s}} \tag{10}$$

Where $\vec{\Psi}_0$ is the initial stator flux before the fault and $\tau_s = L_s / R_s$ is the time constant of the stator. With respect to the rotor windings, this voltage rotates reversely with rotor angular frequency ω_m and has a transient time depending on the machine time constant.

$$\vec{v}_{rn}^{r} = -\frac{L_m}{L_s}\left(\frac{1}{\tau_s} + j\omega_m\right)\vec{\Psi}_0 e^{-\frac{t}{\tau_s}} e^{-j\omega_m t} \tag{11}$$

As the term $1/\tau_s$ is relatively small, the amplitude of the voltage will be:

$$V_{rn} \approx \frac{L_m}{L_s}\frac{\omega_m}{\omega_s}V_s = \frac{L_m}{L_s}(1-s)V_s \tag{12}$$

The induced voltage on the rotor windings during short circuit is similar to stator voltage due to slip constraint range. For super-synchronous speed this voltage can even be higher. Under these short circuit conditions the converter should be able to generate voltage equal to maximum voltage stated in (12) that is very similar to stator-rated voltage, meaning the higher converter size if not the current will be uncontrolled and overcurrent will occur. When generator is subjected to partial voltage dips, Equations (7-12) will have a slight change. Supposing generator is operating in normal condition, at a given moment $t = t_0$ voltage amplitude changes from V_{s1} to V_{s2}. As fluxes are proportional to stator voltages, two different fluxes $\vec{\psi}_{sf1}$ and $\vec{\psi}_{sf2}$ which are also known as forced and natural fluxes respectively, will appear. As mentioned before, the evolution from $\vec{\psi}_{sf1}$ to $\vec{\psi}_{sf2}$ can't be discontinuous, in order to guarantee the continuity, a natural flux which can induce voltages appears. In partial voltage dips the stator flux consists of two fluxes; forced flux which rotates with synchronous angular frequency and the natural flux which is constant

$$\vec{\psi}_s(t) = \vec{\psi}_{sf2} + \vec{\psi}_{sn} = \frac{V_{s2}}{j\omega_s} e^{j\omega_s t} + \frac{V_{s1} - V_{s2}}{j\omega_s} e^{-\frac{t}{\tau_s}} \tag{13}$$

Where $\vec{\psi}_{sf2}$ is the forced flux related to stator voltage changing from V_{s1} to V_{s2} and $\vec{\psi}_{sn}$ is the natural flux. Each of the two terms of (13) induces voltage on rotor, the voltage induced by the forced flux is very similar to the voltage induced during normal operation that is, an AC voltage which is proportional to slip and the stator voltage:

$$\vec{v}_{rf} = V_{s2}\frac{L_m}{L_s} s e^{j\omega_s t} \tag{14}$$

$\vec{v}_{rf}$ is the voltage induced by the forced flux. On the other hand, the natural flux induces voltage that can be calculated from Equation 11:

$$\vec{v}_{rN} = -\frac{L_m}{L_s}\left(\frac{1}{\tau_s} + j\omega_m\right)\frac{V_{s1} - V_{s2}}{j\omega_s} e^{-\frac{t}{\tau_s}} \tag{15}$$

$\vec{v}_{rN}$ is the voltage induced by the natural flux. Due to the small value of $1/\tau_s$, it is possible to rewrite the Equation 15:

$$\vec{v}_{rN} \approx -\frac{L_m}{L_s}\left(\frac{\omega_m}{\omega_s}\right)\left(V_{s1} - V_{s2}\right) e^{-\frac{t}{\tau_s}} \tag{16}$$

By adding (14) and (16) the induced voltage will be expressed as:

$$\vec{v}_{rn} = \vec{v}_{rf} + \vec{v}_{rN} \tag{17}$$

The resultant rotor voltage in a rotor reference frame can be considered as follow:

$$\vec{v}_{rn}^{r} \approx \frac{L_m}{L_s}\left(sV_{s2}e^{j\omega_r t} + (1-s)\left(V_{s1} - V_{s2}\right) e^{-j\omega_m t} e^{-\frac{t}{\tau_s}} \right) \tag{18}$$

The first term of the previous equation is small and is proportional to the slip and its frequency is the difference between the synchronous and the rotor frequencies which will result in low frequency. On the other hand, the second term originates from natural flux, its amplitude is noticeable as it is proportional to the depth of the dip that is $\left(V_{s1} - V_{s2}\right)$and its frequency is the rotor electrical speed ω_m.

2.3. Asymmetrical Voltage Dips

When a fault like single-line-to ground short circuit occurs; the remaining voltages are not the same in the three lines or when short circuits occur between two lines, the phase shift between the three voltages will no longer be 120°. Under these circumstances the faults are considered unbalanced or asymmetrical faults. Symmetrical component method is applied to analyse these types of faults. According to this method the stator voltage can be decomposed as the sum of the positive and negative voltages.

$$\vec{v}_s = \sqrt{2}\underline{V_1}e^{j\omega_s t} + \sqrt{2}\underline{V_2}e^{-j\omega_s t} \tag{19}$$

Where $\underline{V_1}$ and $\underline{V_2}$ are the phasors of positive and negative components of stator voltage space vector. These two voltages create positive and negative fluxes respectively which finally leads to induce voltage on the rotor which can be written as follow in the rotor reference frame:

$$\vec{v}_{r1} = \sqrt{2}\underline{V_1}\frac{L_m}{L_s} s e^{js\omega_s t} \tag{20}$$

$$\vec{v}_{r2} = \sqrt{2}\underline{V_2}\frac{L_m}{L_s}(2-s)e^{-j(2-s)\omega_s t} \tag{21}$$

$$\vec{v}_{rn}^{r} = -\frac{L_m}{L_s} j\omega_m \vec{\psi}_{sn}^{r} \tag{22}$$

$\vec{v}_{r1}$ Is proportional to the slip and its frequency is equal to the slip frequency, $\vec{v}_{r2}$ has higher amplitude than $\vec{v}_{r1}$ and by neglecting "s" its frequency could reach twice the grid frequency. On the other hand, $\vec{v}_{rn}^{r}$ approximately has the grid frequency. Single phase dip is the most common grid fault. Here, it is assumed that short-circuit occurs in phase "a" which causes the voltage in this phase to drop. According to the symmetrical component method if a voltage dip of depth "p" occurs in phase "a"; the positive and negative voltage components of phase "a" cause a negative and positive flux in the stator and also for the continuity of the flux, natural flux will appear. The continuity factor along with the initial conditions of the fluxes, initial natural flux can be achieved:

$$\vec{\psi}_s\left(t_0^-\right) = \vec{\psi}_s\left(t_0^+\right) \tag{23}$$

$$\vec{\psi}_s\left(t_0^-\right) = \vec{\psi}_{s1}\left(t_0^+\right) + \vec{\psi}_{s2}\left(t_0^+\right) + \vec{\psi}_{sn}\left(t_0^+\right) \tag{24}$$

$$\vec{\psi}_{n0} = \vec{\psi}_s^s\left(t_0^-\right) - \vec{\psi}_{s1}^s\left(t_0^+\right) - \vec{\psi}_{s2}^s\left(t_0^+\right) \tag{25}$$

As Equation 25 is a subtraction of complex numbers, the results depend on the phase of the positive and the negative fluxes at t_0^+. In addition different rotating directions of the two fluxes cause the phase shift between them to change over time. This means that the result of (25) is different and depends on the time the voltage dip occurs. To better explain this behaviour, two instants $t_0 = 0$ and $t_0 = T/4$ (T is the grid period) when DFIG is exposed to voltage dips are chosen to be analysed. At $t_0 = 0$, at this moment because of aligned positive and negative fluxes and their summation which is equal to the flux before the fault, results in zero natural flux, so the stator flux remains in the steady state. Equations describing the positive and negative fluxes at this moment are (with $\hat{V}_{pre}$ being the stator voltage before voltage dip):

$$\vec{\psi}_s^s\left(0^-\right) = \frac{\hat{V}_{pre}}{j\omega_s} \tag{26}$$

$$\vec{\psi}_s^s\left(0^+\right) = \frac{\hat{V}_{pre}\left(1-\frac{p}{3}\right)}{j\omega_s} + \frac{-\hat{V}_{pre}\frac{p}{3}}{-j\omega_s} = \frac{\hat{V}_{pre}}{j\omega_s} \tag{27}$$

In $t_0 = T/4$ at this moment because of the opposed positive and negative fluxes and their destructive summation the natural flux initial value is the largest. The initial value of the natural flux can be calculated as follow:

$$\vec{\psi}_s^s\left(\frac{T^-}{4}\right) = \frac{\hat{V}_{pre}}{j\omega_s} \tag{28}$$

$$\vec{\psi}_s^s\left(\frac{T^+}{4}\right) = \frac{j\hat{V}_{pre}\left(1-\frac{p}{3}\right)}{j\omega_s} + \frac{j\hat{V}_{pre}\frac{p}{3}}{-j\omega_s} + \vec{\psi}_{n0} \tag{29}$$

$$\vec{\psi}_{n0} = \frac{\hat{V}_{pre}\frac{2}{3}p}{\omega_s} \tag{30}$$

When a short circuit between two phases occurs, their voltages get closer in value and the voltage of the unfaulty phase remains the same if it is assumed that the positive and the negative sequence networks have equal impedance. Compared to single-phase, the phase-phase faults cause a larger negative sequence in the voltage for the same depth. Just as in single-phase fault, two instants $t_0 = 0$ and $t_0 = T/4$ will be considered to calculate the initial natural flux. At $t_0 = 0$ because of the opposing positive and negative fluxes, the largest natural flux arises in the stator which can be expressed by the following equation:

$$\vec{\psi}_{sn}\left(0^+\right) = \psi_{n0} = \frac{\hat{V}_{pre}}{j\omega_s}p \tag{31}$$

At $t_0 = T/4$, Equality between the addition of the positive and negative fluxes and prefault flux will result in zero natural flux, with no natural flux no induced voltage is induced, that is the rotor voltage is smaller.

3. DYNAMIC VOLTAGE RESTORER (DVR)

To overcome the aforementioned voltage dips problems, DVR can be the best economical and technical solution. Several articles on this topic have addressed applying DVRs [16-19, 29]. In the previous papers, as mentioned, the existing of energy storage elements in DVR is considered as a disadvantage, such as no long time voltage compensating, higher cost and volume, limited application. The proposed DVR consists of three independent three-phase to single-phase direct converters which can operate independently. As each converter operates independently and the compensation voltage for any faulty phase or phases is taken from all three phase or phases, the proposed DVR can operate regardless of the fault type and can compensate just the faulty phase (or phases). Moreover, no dc-link results in long time compensation and considerable reduction in cost and physical volume. In addition an injection transformer with a turns ratio of 1: a (a for grid side), an LC filter, a bypass switch (to bypass the DVR under normal operation) are used. Figure 2 shows the schematic diagram of one of the three independent converters, the other two converters are the same. The common-emitter antiparallel IGBTs with a diode-pair arrangement have been utilized for the purpose of this paper and all these switches are assumed to be ideal. By applying DVR to a DFIG, the voltage across the stator becomes:

$$v_s(t) = v_g(t) + v_{inj}(t) \tag{32}$$

Where $v_s(t)$, $v_g(t)$ and $v_{inj}(t)$ are the instantaneous stator, grid and DVR injected voltages, respectively. Under normal operations, DVR is bypassed by closing the switch "K". High frequency pulse width modulation is applied to the DVR in order to control the used converters. Each sampling period consists of two time intervals $t_{\max}$ and t_{zero}. For example for the nth sampling period of T_s:

$$T_s = t_{\max}^n + t_{zero}^n \tag{33}$$

During t_{zero} time interval, switches that cause zero voltage generation at the converter output side will be turned on and for the $t_{\max}$, depending on the converter output voltage, switches that cause maximum absolute output voltage generation will be turned on, that is, maximum positive voltage if the converter output voltage is in its positive half cycle and maximum negative output voltage if the converter output voltage is in its negative half cycle. So it can be concluded that in each sampling period, two voltages $v_{\max}$ and $v_{zero} = 0$ will appear in the converter output. To describe the switching procedure, the first phase ("a")

is analysed here, the procedure for the other two phases are the same. Considering Figure 3 and Table 1, switching sequence can be achieved:

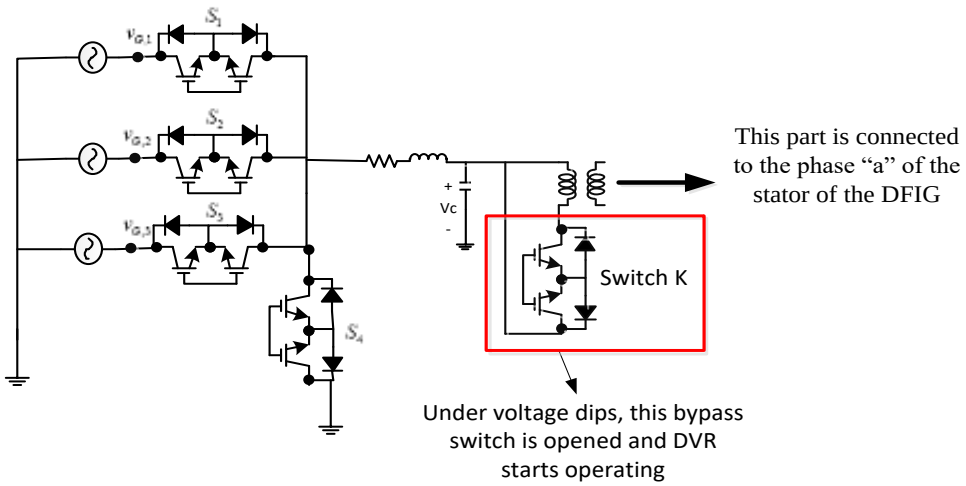

Figure 2. One of the three independent converters used in DVR

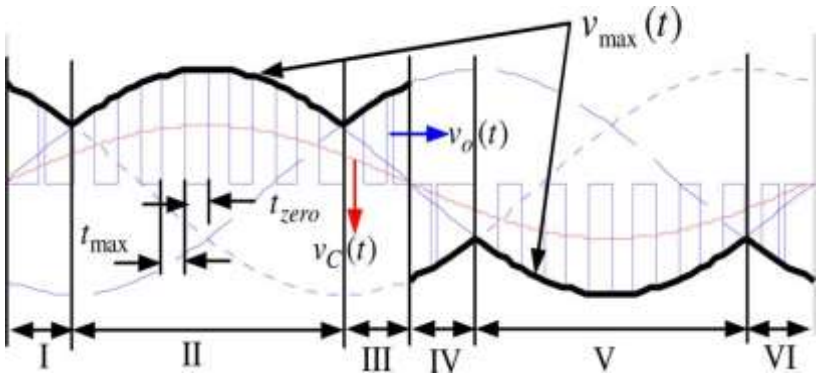

Figure 3. Modulation method applied to the converters used in DVR [30]

Table 1. Different Modes of Operation along with Their Switches States and v_{max}[30]

Mode of Operation	v_{max}	On switches	
		t_{max}	t_{zero}
I, IV	$v_{G,3}$	S_3	S_4
II, V	$v_{G,1}$	S_1	S_4
III, VI	$v_{G,2}$	S_2	S_4

4. SIMULATION

In order to validate the efficacy of the proposed DVR system, both symmetrical and asymmetrical voltage dips are applied to the DFIG. After applying DVR, simulations verifies the improvements of the DFIG operation under symmetrical and asymmetrical voltage dips. As long as the DFIG wind turbine system is protected by DVR, overcurrent and overvoltage will decay and the converter of DFIG remains in operation. The simulations have been performed by PSCAD/EMTDC and the results show that DFIG can be completely protected. the common emitter configuration are considered for the switches which consists of two common emitter insulated-gate bipolar transistors(IGBTs) with two antiparallel diodes and are assumed

to be ideal. In the normal operation the stator of the DFIG is connected to the grid through a DVR and its voltage is 220 $Vrms$ (L-G). The switching frequency of DVR is 6 kHz and the grid frequency is50 Hz. Initially, the system is in steady state until a voltage dip occurs in t=1s and recovers in t=1.1s. The passive LC filter with damping resistor used in DVR are $L = 8\,mH, C = 11\,\mu F$ and$R = 0.1\,\Omega$. For the DFIG part, the parameters are indicated in Table 2.

As the depth of the voltage dip is assumed equal to each phase with no phase jump thus this condition can be considered as a three-phase voltage dip. Each phase of the grid is subjected to a voltage dip with depth of 40%. Figure 7 illustrates the behaviour of grid voltages, DVR voltage and the stator voltage of the DFIG under symmetrical and asymmetrical voltage dips. It can be seen from the figure that voltage dip occurs at t=1s and lasts for 0.1s. Stator and rotor currents along with the active and reactive powers of the DFIG wind turbine with and without compensation are shown in Figure 8. Applying DVR provides condition for DFIG-based wind turbines to continue its normal operation while subjected to voltage dips.

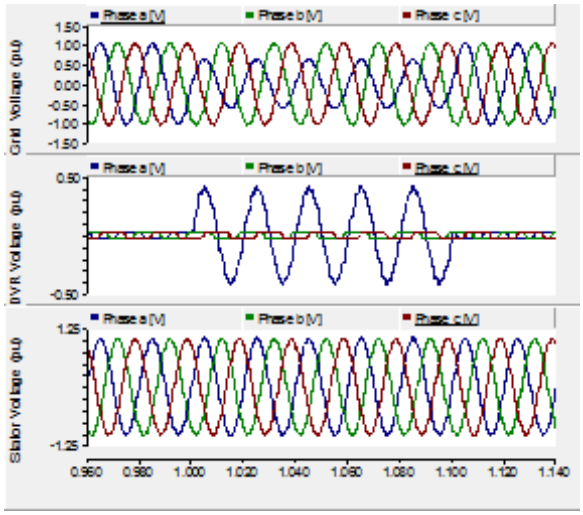

(a)

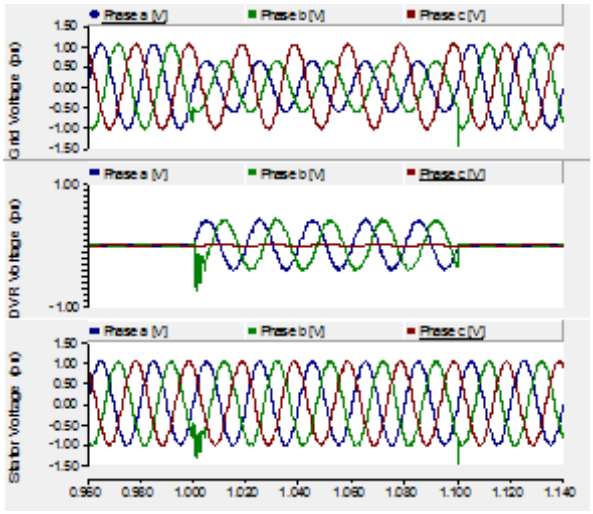

(b)

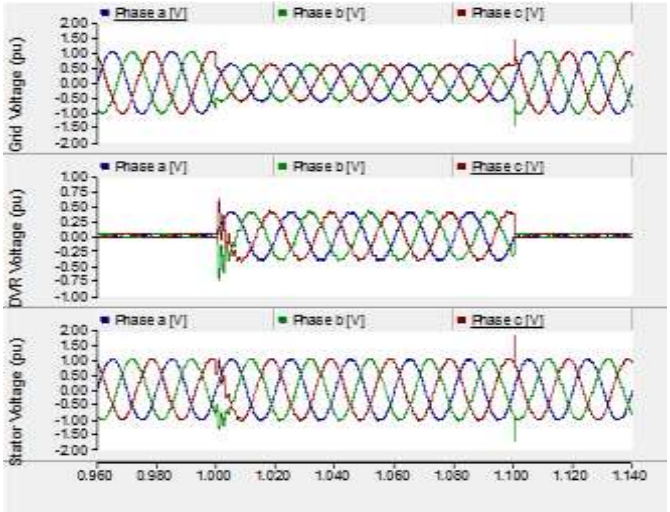

(C)

Figure 7. From top to bottom, grid voltage, DVR injected voltage and stator voltage under 40% of: (a)single phase voltage dip, (b) phase-phase voltage dip and (c) three phase voltage dip active and reactive power of DFIG

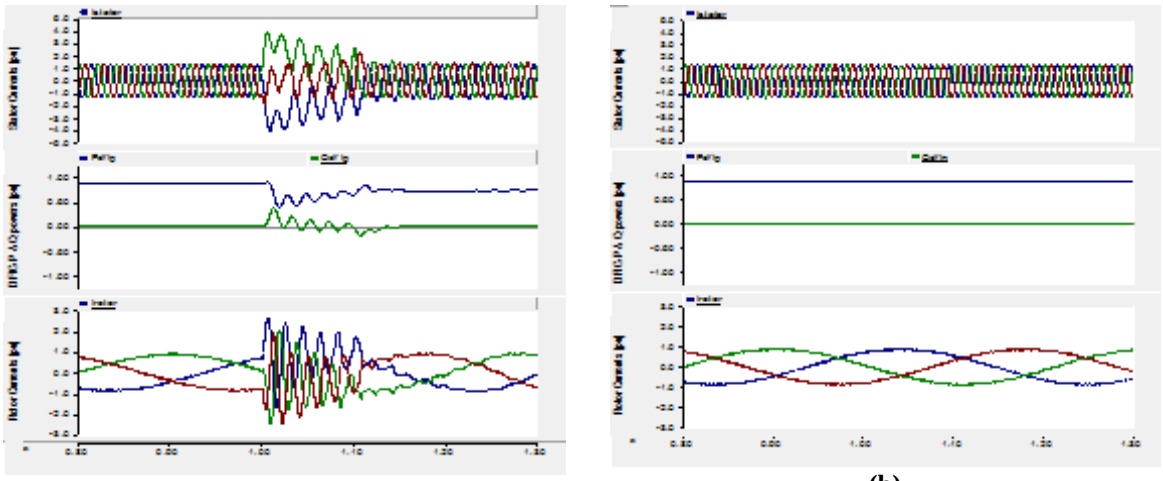

(a) **(b)**

Figure 8. From top to bottom, stator currents, DFIG active and reactive powers and rotor currents under 40% of three phase voltage dip: (a) without compensation and (b) with DVR compensation

5. CONCLUSION

A new dynamic LVRT solution for DFIG-based wind turbines is presented. A DVR topology without any energy storage element, based on three phase to single phase direct converters is utilized to compensate voltage dips that occur in grid networks which cause high currents in the converter of DFIG that can saturate or destroy it. The injected voltages of DVR are a combination of the voltages of the three phases which result in independent operation of three direct converters and as mentioned, because of no dc-link; long-term compensation, a great decrease in cost, weight, and volume is obtained. By applying the DVR, the LVRT capability of DFIG-based wind turbines are improved and the stable operation of DFIGs are guaranteed. The behaviour of DFIG and DVR under three-phase, phase-phase, and single phase voltage dips with the depth of 40% are simulated which show the effectiveness of the DVR system improving the LVRT capability of DFIG.

REFERENCES

[1] Blaabjerg, F., & Ma, K. (2013). Future on power electronics for wind turbine systems. *IEEE Journal of Emerging and Selected Topics in Power Electronics*, 1(3), 139-152.

[2] Anaya-Lara, O., Jenkins, N., Ekanayake, J., Cartwright, P., & Hughes, M. (2011). Wind energy generation: modelling and control. John Wiley & Sons.

[3] Murthy, S. S., Singh, B., Goel, P. K., & Tiwari, S. K. (2007, November). A comparative study of fixed speed and variable speed wind energy conversion systems feeding the grid. *In 2007 7th International Conference on Power Electronics and Drive Systems (pp. 736-743). IEEE.*

[4] Justo, J. J., Mwasilu, F., & Jung, J. W. (2015). Doubly-fed induction generator based wind turbines: A comprehensive review of fault ride-through strategies. *Renewable and Sustainable Energy Reviews*, 45, 447-467.

[5] Kimura, N., Hamada, T., Sonoda, M., Morizane, T., Taniguchi, K., & Nishida, Y. (2009, May). Suppression of current peak of PFC converter connected to induction generator for wind power generation excited by voltage source converter. *In Power Electronics and Motion Control Conference, 2009. IPEMC'09. IEEE 6th International (pp. 2269-2274). IEEE.*

[6] Brekken, T., & Mohan, N. (2003, June). A novel doubly-fed induction wind generator control scheme for reactive power control and torque pulsation compensation under unbalanced grid voltage conditions. *In Power Electronics Specialist Conference, 2003. PESC'03. 2003 IEEE 34th Annual(Vol. 2, pp. 760-764). IEEE.*

[7] Blaabjerg, F., & Chen, Z. (2005). Power electronics for modern wind turbines.Synthesis Lectures on Power Electronics, 1(1), 1-68.

[8] Ananth, D. V. N., & Kumar, G. N. (2016). Performance Evaluation of DFIG During Asymmetrical Grid Disturbances Using Internal Model Controller and Resonant Controller. *International Journal on Electrical Engineering and Informatics, 8(3), 494.*

[9] Abad, G., Lopez, J., Rodriguez, M., Marroyo, L., & Iwanski, G. (2011). Doubly fed induction machine: modeling and control for wind energy generation (Vol. 85). John Wiley & Sons.
[10] Sun, T., Chen, Z., & Blaabjerg, F. (2003, November). Voltage recovery of grid-connected wind turbines after a short-circuit fault. In Industrial Electronics Society, 2003. IECON'03. *The 29th Annual Conference of the IEEE (Vol. 3, pp. 2723-2728). IEEE.*
[11] Awad, H., Svensson, J., & Bollen, M. (2004). Mitigation of unbalanced voltage dips using static series compensator. *IEEE Transactions on Power Electronics*, 19(3), 837-846.
[12] Nunes, M. V., Lopes, J. P., Zurn, H. H., Bezerra, U. H., & Almeida, R. G. (2004). Influence of the variable-speed wind generators in transient stability margin of the conventional generators integrated in electrical grids. *IEEE Transactions on Energy Conversion, 19(4), 692-701.*
[13] Peng, L., Francois, B., & Li, Y. (2009, February). Improved crowbar control strategy of DFIG based wind turbines for grid fault ride-through. *In Applied Power Electronics Conference and Exposition, 2009. APEC 2009. Twenty-Fourth Annual IEEE (pp. 1932-1938). IEEE.*
[14] Dami, M. A., Jemli, K., Jemli, M., & Gossa, M. (2010). Doubly fed induction generator, with crow-bar system, under micro-interruptions fault. *International Journal on Electrical Engineering and Informatics*, 2(3), 216.
[15] Vidal, J., Abad, G., Arza, J., & Aurtenechea, S. (2013). Single-phase DC crowbar topologies for low voltage ride through fulfillment of high-power doubly fed induction generator-based wind turbines. *IEEE Transactions on Energy Conversion, 28(3), 768-781.*
[16] Wessels, C., Gebhardt, F., & Fuchs, F. W. (2011). Fault ride-through of a DFIG wind turbine using a dynamic voltage restorer during symmetrical and asymmetrical grid faults. *IEEE Transactions on Power Electronics, 26(3), 807-815.*
[17] Ramirez, D., Martinez, S., Platero, C. A., Blazquez, F., & de Castro, R. M. (2011). Low-voltage ride-through capability for wind generators based on dynamic voltage restorers. *IEEE Transactions on Energy Conversion, 26(1), 195-203.*
[18] Ibrahim, A. O., Nguyen, T. H., Lee, D. C., & Kim, S. C. (2011). A fault ride-through technique of DFIG wind turbine systems using dynamic voltage restorers. *IEEE transactions on energy conversion, 26(3), 871-882.*
[19] Sivasankar, G., & Kumar, V. S. (2015). Vector Control Based Dynamic Voltage Restorer for Fault Ride Through of Doubly Fed Induction Generator. *In Power Electronics and Renewable Energy Systems (pp. 1331-1338). Springer India.*
[20] Rolan, A., Corcoles, F., & Pedra, J. (2012). Behaviour of the doubly fed induction generator exposed to unsymmetrical voltage sags. *IET electric power applications, 6(8), 561-574.*
[21] Mohseni, M., Islam, S. M., & Masoum, M. A. (2011). Impacts of symmetrical and asymmetrical voltage sags on DFIG-based wind turbines considering phase-angle jump, voltage recovery, and sag parameters. *IEEE Transactions on power electronics, 26(5), 1587-1598.*
[22] Marques, G. D., & Sousa, D. M. (2012). Understanding the doubly fed induction generator during voltage dips. *IEEE Transactions on Energy Conversion, 27(2), 421-431.*
[23] Nian, H., Song, Y., Zhou, P., & He, Y. (2011). Improved direct power control of a wind turbine driven doubly fed induction generator during transient grid voltage unbalance. *IEEE Transactions on Energy Conversion, 26(3), 976-986.*
[24] Zhou, P., He, Y., & Sun, D. (2009). Improved direct power control of a DFIG-based wind turbine during network unbalance. *IEEE Transactions on Power Electronics, 24(11), 2465-2474.*
[25] Abad, G., Rodriguez, M. A., Iwanski, G., & Poza, J. (2010). Direct power control of doubly-fed-induction-generator-based wind turbines under unbalanced grid voltage. *IEEE Transactions on Power Electronics, 25(2), 442-452.*
[26] Xu, L. (2008). Coordinated control of DFIG's rotor and grid side converters during network unbalance. *IEEE Transactions on Power Electronics, 23(3), 1041-1049.*
[27] Santos-Martin, D., Rodriguez-Amenedo, J. L., & Arnaltes, S. (2009). Providing ride-through capability to a doubly fed induction generator under unbalanced voltage dips. *IEEE Transactions on Power Electronics, 24(7), 1747-1757.*
[28] Lopez, J., Sanchis, P., Roboam, X., & Marroyo, L. (2007). Dynamic behavior of the doubly fed induction generator during three-phase voltage dips. *IEEE TRANSACTIONS ON ENERGY CONVERSION EC, 22(3), 709.*
[29] Abdel-Baqi, O., & Nasiri, A. (2009, November). A dynamic LVRT solution for doubly-fed induction generator. In Industrial Electronics, 2009. *IECON'09. 35th Annual Conference of IEEE (pp. 825-830). IEEE.*
[30] Babaei, E., Kangarlu, M. F., & Sabahi, M. (2010). Mitigation of voltage disturbances using dynamic voltage restorer based on direct converters. *IEEE Transactions on Power Delivery, 25(4), 2676-2683.*

BIOGRAPHIES OF AUTHORS

Kiarash Azizi was born in Urmia, Iran in Septambr 1988. He received B.Sc. degree in power Electrical Engineering from University of Urmia, Urmia, Iran. He is now a Master student in Urmia University,. His main research interests are about Renewable Energies Electric vehicles, FACTS and power Electronics in general.

Murteza Farsadi was born in Khoy, Iran in Septambr 1957. He received B.Sc. degree in Electrical Engineering M.Sc. degree in Electrical and Electronics Engineering and Ph.D. degree in Electrical Engineering (High voltage) from Middle East Technical University (METU), Ankara, Turkey in 1982, 1984, and 1989, respectively. He is now an associate professor in Electrical Engineering Department of Urmia University, Iran. His main research interests are in high voltage engineering, industrial power system studies, FACTS, HVDC transmission systems, DC/AC active power filters, renewable energy, hybrid and electrical vehicles, and new control methods.

Mohammad Farhadi Kangarlu was born in Kangarlu, Iran, in 1987. He received the B.S. degree in electrical engineering from the University of Tabriz, Tabriz, Iran, in 2008. His research interests include power quality, power-electronic converters, and custom power devices.